Detecting Epileptic Seizures in Long-term Human EEG: A New Approach to Automatic Online and Real-Time Detection and Classification of Polymorphic Seizure Patterns

Ralph Meier,†‡ Heike Dittrich,† Andreas Schulze-Bonhage,†‡ and Ad Aertsen*‡*

Summary: Epileptic seizures can cause a variety of temporary changes in perception and behavior. In the human EEG they are reflected by multiple ictal patterns, where epileptic seizures typically become apparent as characteristic, usually rhythmic signals, often coinciding with or even preceding the earliest observable changes in behavior. Their detection at the earliest observable onset of ictal patterns in the EEG can, thus, be used to start more-detailed diagnostic procedures during seizures and to differentiate epileptic seizures from other conditions with seizure-like symptoms. Recently, warning and intervention systems triggered by the detection of ictal EEG patterns have attracted increasing interest. Since the workload involved in the detection of seizures by human experts is quite formidable, several attempts have been made to develop automatic seizure detection systems. So far, however, none of these found widespread application. Here, we present a novel procedure for generic, online, and real-time automatic detection of multimorphologic ictal-patterns in the human long-term EEG and its validation in continuous, routine clinical EEG recordings from 57 patients with a duration of approximately 43 hours and additional 1,360 hours of seizure-free EEG data for the estimation of the false alarm rates. We analyzed 91 seizures (37 focal, 54 secondarily generalized) representing the six most common ictal morphologies (alpha, beta, theta, and delta- rhythmic activity, amplitude depression, and polyspikes). We found that taking the seizure morphology into account plays a crucial role in increasing the detection performance of the system. Moreover, besides enabling a reliable (mean false alarm rate <0.5/h, for specific ictal morphologies <0.25/h), early and accurate detection (average correct detection rate $>96\%$) within the first few seconds of ictal patterns in the EEG, this procedure facilitates the automatic categorization of the prevalent seizure morphologies without the necessity to adapt the proposed system to specific patients.

Key Words: Long-term human EEG, Seizure detection, Ictal morphology categorization, Polymorphic seizure patterns, Support Vector Machines.

(*J Clin Neurophysiol* 2008;25: 000–000)

Epileptic seizures are caused by excessive, synchronized activity of large groups of neurons. Among the wide spectrum of mechanisms leading to such a pathologic activation are structural malformations of the cerebral cortex, brain injuries of various types, and physiological conditions leading to changes in network excitability. Depending on the localization and extent of ictal epileptic activity, epileptic seizures can cause a variety of temporary changes in perception and behavior. The most important tool for the diagnosis of epilepsy is the EEG, in which epileptic seizures become apparent as characteristic, usually rhythmic signals, often coinciding with or even preceding the earliest observable changes in behavior. Their detection can, thus, be used to react to an impending or ongoing seizure, or to differentiate epileptic seizures from other conditions with paroxysmal, seizure-like symptoms.

Because of the large numbers of patients with epilepsy and the considerable workload involved in the detection of seizures by human experts, several attempts have been made to develop automatic seizure detection systems. The seminal work of Gotman (1982) first mentions the problem of polymorphic seizure types and the resulting difficulties for detection systems. Here, we present a novel system and associated signal analysis procedures for online, real-time automatic seizure detection, and seizure type classification in the human EEG. We show results of the validation of the new system for aiding diagnosis in routine clinical application, based on a newly developed, large benchmark data set of long-term EEG recordings. The categorization of different seizure morphologies is performed on the basis of the associated polymorphic ictal patterns. Finally, we show advantages of combining multiple features for detecting ictal epochs in the EEG and the impact of different seizure morphologies on detection performance and latency.

From the *Neurobiology and Biophysics, Faculty of Biology, Albert-Ludwigs-University, Freiburg, Germany; †Epilepsy Center, University Hospital, Freiburg, Germany; and ‡Bernstein Center for Computational Neuroscience Freiburg, Albert-Ludwigs-University, Freiburg, Germany.

Partial funding for this research was supplied by the Committee for Research, University Clinics, Freiburg and the German Federal Ministry for Education and Research (BMBF, grant 01GQ0420 to BCCN Freiburg).

Address correspondence and reprint requests to: Ralph Meier, Neurobiology and Biophysics, Institute of Biology III, Albert-Ludwigs-University, Schänzlestrasse 1, D-79104 Freiburg i.Br., Germany. e-mail: meier@biologie.uni-freiburg.de.

ISSN: 0736-0258/08/2503-0001

METHODS

Several tools and methods for mapping seizure features to clinically relevant parameters and for describing preseizure changes in the EEG and the ECoG have been described in the literature (cf. review by Gotman, 1999). Also, there are many well-known seizure detection algorithms for both, scalp and intracranial recordings (e.g., Le Van Quyen et al., 1999, 2000, 2001; Murro, 1991, Sharbrough, 1993; Osorio et al., 1998, 2002). However, although ictal EEG patterns are polymorphic, we are not aware of any study taking the different seizure morphologies into account in the detection. The review of McSharry et al. (2002) offers an excellent overview of the various linear and nonlinear methods for automatic seizure detection in scalp EEG recordings. All approaches mentioned there contributed substantially to increasing our understanding of the seizure detection problem and to the general understanding of epileptiform activity in the human EEG. In the following, we give a brief overview of these different approaches and their characteristics, focusing on the issues that are relevant for the present article.

Linear and Nonlinear Methods

One of the simpler linear features described is the variance of the EEG signal. Unfortunately, changes in the variance of the EEG might be caused by a variety of activity patterns in the brain, comprising different seizure types, changes in mental state (e.g., sleep stages), and even artifacts. One of the other well-established methods is the continuous wavelet transformation (CWT) (Daubechies, 1994). Any continuous function may be uniquely projected onto the wavelet basis functions and expressed as a linear combination of these. The collection of coefficients (weight functions) representing an arbitrary continuous signal in terms of the wavelet basis functions is referred to as the Wavelet Transform of the given signal. The strength of the wavelet transform representation is that signals that "look like" a wavelet function at any scale are well represented by only few wavelet coefficients. The wavelet transform, therefore, provides an efficient representation for functions that have similar characteristics as the wavelet basis functions. In contrast to the Fourier expansion, the wavelet decomposition offers a compact support. This means that the basis functions are nonzero only on a finite time interval. By contrast, the sinusoidal basis functions of the Fourier expansion are infinite in extent. Therefore, the CWT does not only measure the frequency content of a signal, but also its temporal position and extent, hence it is used in many biologic signal applications (e.g., Ishikawa and Mochimaru, 2002; Schiff et al., 1994). CWT has been applied for seizure detection on intracerebral data with impressive success, for example by Kahn and Gotman (2003). Other methods for measuring the amount of ictal activity in an EEG signal are based on elaborate filters and measurements of the residual signal energy. One such filter is the median filter, used in a study by Echauz et al. (1999), which is suited to reduce noise and high-frequency oscillations in signal data and, thereby, leads to a robust measurement of the overall signal wave trend.

To the best of our knowledge, there is no up-to-date study that quantifies the performance of a seizure detection system based on median-filtered EEG signals by its evaluation on a data set of EEG data where seizure-morphologies are described and taken into account. Moreover, most algorithms implemented so far did not focus on pathophysiological phenomena characteristic for epileptic activity, such as changes in synchronization and correlation of EEG signals from different brain areas (e.g., Bikson et al., 2003; Netoff and Schiff, 2002). Surface EEG does reflect (at least part of) these changes in brain dynamics, which may be useful for the purpose of seizure detection and pattern classification. We, thus, considered the information accumulated from several different EEG features as potentially useful to discriminate between ictal and normal EEG, especially in recordings containing considerable amounts of artifacts. Since multiple models for the origin and maintenance of ictal activity exist, we tried to capture potential effects of these various neuronal activity patterns in the surface EEG by using multiple extracted features. For a motivation of the individual features used in our study, we refer to Features section.

Several studies proposed to quantify nonlinear correlations in the EEG signal to describe ictal activity (Le van Quyen et al., 1999, 2000, 2001). While recently the usefulness of linear methods has come under debate (McSharry, 1999), they nevertheless remain widely used. Known drawbacks of using nonlinear features are the nonintuitive nature of such measures, the large amount of data needed for reliable parameter estimation including issues of stationarity within these epochs, and the high computational demand. These disadvantages prevent applications with short latency with regard to recording time, and might cause problems in real-time applications. Thus, despite the potential superiority of nonlinear features in reflecting ictal activity, we focused on linear methods for feature analysis for our present purpose.

EEG Data

All data used here were gathered during routine presurgical diagnosis in the Center for Epilepsy at the University Hospital Freiburg, Germany. Clinical data and corresponding EEG recordings were stored in a database (Dittrich et al., 2003). The present study is based on a set of 91 seizures recorded in 57 patients, selected to cover all major ictal seizure morphologies, i.e., rhythmic activities in the alpha-, beta-, theta- and delta-bands, amplitude depression, and runs of polyspikes (cf. Sharbrough, 1993). Data were continuously recorded using standard clinical recording systems (IT-Med GmbH, Usingen, Germany) with electrode placement according to the international 10–20 system; the entire recordings were reviewed by certified electroencephalographers. An overview of the data analyzed in the present study is given in Table 1. The respective morphology at seizure onset was classified by the electroencephalographers. We collected the data such as to sample the spectrum of seizure types with an approximately equal number of seizures for each type, aiming for as many different patients per seizure type as possible. No further criteria for selection (e.g., general recording quality or whether the initial ictal pattern was representative for its class) were used. The seizure onset was defined as the beginning of the first observable seizure pattern in the EEG. Depending on the epileptogenic zone and on the pattern of

TABLE 1. Summary of the Properties of the EEG Data Set (~43 h) Containing 91 Seizures Recorded in 57 Patients, Representing 6 Morphologies, Used in the Present Study

Initial Morphology	No. Seizures	Percentage of Total No. Seizures [%]	Average No. Seizures Per Patient ± SD	No. Focal/ Generalized Seizures	Duration of Initial Ictal Pattern (±SD)	No. Patients Contributing Seizures	Analyzed EEG Data [min]
Rhytmic alpha activity	15	16.5	1.3 ± 0.6	10/5	11.5 ± 5	12	410
Rhytmic beta activity	19	20.9	2.4 ± 2.8	6/13	8.2 ± 4.5	8	465
Rhytmic theta activity	17	18.6	1.1 ± 0.3	11/6	11.7 ± 4.9	16	503
Rhytmic delta activity	16	17.6	1.1 ± 0.3	10/6	9.4 ± 4.7	15	443
Amplitude depression	12	13.2	4.0 ± 2.6	0/12	6.8 ± 3.7	3	219
Poly spikes	12	13.2	1.3 ± 0.7	0/12	4.3 ± 3.3	9	531
Summary	91	100	1.6	37/54	8.8	57	2571

The data presented in this table was used for the detailed analysis shown throughout this article. To confirm the false alarm rate, we additionally analyzed approximately 24 h seizure-free data from each of the 57 patients used here. This results in roughly 1,400 h of seizure-free EEG data evaluated.

spread to symptomatogenic zones and to the lateral convexity of the brain, initial seizure patterns may precede or follow changes in patient behavior. For each of the 91 seizures in the database, we used the EEG recordings before seizure onset and included only data after the offset of the preceding seizure as nonictal activity (see Table 1 for details). Furthermore, the false alarm rate of the proposed detection system was confirmed by analyzing approximately 24 hours seizure-free data from the same subset of patients (in total equaling over 1,400 hours seizure-free EEG data). This 24 hours seizure-free data set was neither used for calibration nor for method development. It was only used in the final validation step to confirm the false alarm rate estimated on the short dataset described in Table 1.

Seizures can be defined as "subclinical" when only the EEG pattern changes in a characteristic way, without an observable change in patient behavior. Such seizures were not used as seizure examples, but their occurrence during interictal EEG epochs cannot be fully excluded. Generally, the full EEG was reviewed to determine when seizures occurred and additionally the video was reviewed to determine which had clinical signs. For the definition of the onset of the initial ictal pattern only the EEG was reviewed. Neither video nor other information sources were used by the medical personnel for this task. The duration of the initial ictal patterns are shown in Table 1.

Features

Seven features were derived from continuously recorded surface EEG data (sampled at 256 Hz) for quantifying the ictal activity. Each single feature results in one value for an epoch of 1 second (corresponding to 256 samples of EEG data), combining standard channels (Fp1, Fp2, F3, F4, C3, C4, P3, P4, O1, O2, F7, F8, T3, T4, T5, T6, Fz, Cz, Pz) from the international 10–20 system and, if available, also the two sphenoidal (Sp1, Sp2) channels. The analysis window was moved in steps of 128 samples, i.e., half a second, over the data. A common average montage was selected for automated EEG analysis. The raw EEG data were filtered in different ways to preprocess it for feature extraction. One type of filter was a third order Butterworth bandpass filter between 2 and 42 Hz. From here on, this filter will be referred to as bandpass, or BP. The two other filters used were Savitzky-Golay filters (Press et al., 1992) with a width of nine samples each. One was a smoothing filter, the other a first order derivative filter. These filters will be referred to as SG0 and SG1, respectively.

A brief overview of the features used in this study is given in Table 2. A more-detailed definition of each feature and a description how it was obtained is given in the following.

Continuous Wavelet Transform

Wavelets were introduced for seizure description in the surface EEG by Battiston et al. (2003), their inherent properties make them ideally suited to capture short epochs of oscillations or reverberations in multiple frequency ranges (D'Arcangelo et al., 2002; Dzhala and Staley, 2003). Here, we chose the Symlet 5 wavelets of scale 25 and 32 as CWT

TABLE 2. Summary of Features and Abbreviations Used in the Present Study

No.	Abbreviation	Brief Description	Feature Rank
1	CTW 25	Power of CWT with Symlet 5 of Scale 25	3
2	CWT 32	Power of CWT with Symlet 5 of Scale 32	4
3	Mean Var	Mean sliding variance	2
4	Mean CC	Mean cross correlation coefficient	1
5	Sav0	Power after smoothing with SG0 filter	6
6	SavM	As Sav0, with additional floating mean filtering	7
7	ZeroX	No. zero-crossings in derivative SG1 filtered signal	5

Features similar to Nos. 1, 2 and 3 were already used in earlier seizure-detection studies (Osorio et al., 2002; Esteller et al., 1999a; McSharry et al., 2002), however, mostly for intracranial data. In addition, we define here the new features 4 to 7, which are used here for seizure detection for the first time.

Moreover, we show the rank of the features according to their performance in seizure detection with a linear thresholding algorithm. Feature No. 4 (mean CC) performs best, while No. 6 (SavM) seems to be less important in a single feature based, linear seizure detection approach (c.f. also Feature Ranking Using Linear Classifiers section).

features (Nos. 1 and 2 in Table 2). For extraction of these two features, the bandpass-filtered data were used. For each channel, the wavelet transformation was performed and the total signal energy over 256 samples, including all channels, was determined.

Mean Sliding Variance

The sliding power estimation was introduced for seizure detection by Esteller et al. (1999). This measure captures temporal changes in the EEG power, irrespective of the underlying spectral distribution. We calculated the sliding variance (No. 3 in Table 2) with one sample step width for each EEG channel, and averaged across channels to obtain the mean power.

Mean Cross Correlation

For this feature (No. 4 in Table 2), we computed the mean of all pairwise cross correlations (excluding auto correlations), summarized as

$$\text{mean CC} = \frac{2}{N(N-1)} \sum_{i \neq j} x_i x_j,$$

where N is the number of channels, i and j are the channel indices, and x_i and x_j are the respective channel signals. Such measurement can detect electrode crosstalk and, even more important, measure the spatial spread of synchronized activity, which should be especially relevant for generalized seizures, as they are expected to be reflected on more than one electrode.

Savitzky-Golay Filter

It has been suggested that the median-filtered signal power is a good measure for quantifying the amount of ictal activity in the signal (Echauz et al., 1999). Here, we used filtering with a floating mean, instead, because median-filtering is computationally quite intensive. To this end, the raw EEG signal was filtered with a smoothing SG0 filter (No. 5 in Table 2), and additionally filtered with a floating mean filter with a width of 256 samples (No. 6 in Table 2). The power of the resulting signal was then obtained using the standard bin width. Savitzky-Golay (Press et al., 1992) FIR low-pass filters can be thought of as a generalized moving average. Their coefficients are chosen such as to preserve higher moments in the data, thereby reducing the distortion of essential features in the spectrum (peak heights, line widths), while maintaining the efficacy of the random noise suppression.

Zero-Crossings

Counting zero-crossings is a very simple (and computationally cheap) way to assess the dominant frequency of a signal. Examining EEG frequency was among the earliest approaches to automatic seizure detection (Murro, 1991). For this feature (No. 7 in Table 2), we determined the total number of zero crossings over all channels. We found it useful to filter the EEG signal beforehand with the SG1 derivative filter to provide more artifact robustness, mainly because it reduces low frequencies and effectively detrends the signal.

Normalization

Normalization of data has two major goals. The first—and more obvious—is to discard the individual, patient-dependent baseline, to make measurements comparable across patients. The second—and more subtle—is to obtain a sparse, easy to use value distribution, allowing the classifier [e.g., a Support Vector Machine (SVM)] to generate an efficient model and to develop good generalization ability. Here, we normalized each sample of a feature vector separately by replacing it with a measure for its change over the recent past. This change is exploited here for seizure detection, since an emerging seizure will be reflected by changes in the feature values. Specifically, for each sample we compared its recent history (past 5 seconds) with a baseline, consisting of its longer-term history (past 25 seconds). These two time series were compared by a floating rank sum test (Wilcoxon), yielding the probability of having identical value distributions in the two time series. This transformation results in a mapping of the feature value space into a P value space for each feature, normalized according to the probability of observing a change within the previously described time window. We used the output of the Wilcoxon test (the P value) for each of the seven features combined into a 7D P value time series as input for the SVM.

Feature Value Distributions and Optimizations

The features used here were optimized using an iterative procedure. In a first step, we tested for each of the seven selected features (cf. Table 2) separately, how well it separated ictal from nonictal activity for each of the six seizure morphologies (cf. Table 1). This first step was performed on a subset of the data, containing 37 (of 91) seizures, with seizure morphology distribution similar to the entire set. To measure the potential separability of each of the seizure morphologies in the data subset by any one feature, we used the k-factor

$$k = \frac{|m_1 - m_2|}{\sqrt{(v_1 + v_2)/2}} \text{ (Esteller, 1999),}$$

where m_1, m_2 denote the means and v_1, v_2 the variances of the selected feature values for this particular seizure morphology for the two classes (ictal vs. nonictal). The mean k-factor over all morphologies was then maximized during a calibration phase on the data subset, by varying the selection of features and their parameter settings (cf. Table 2). Then, in a second step, we computed a Self Organizing Map (SOM, see e.g., Alhoniemi et al., 2001; Kohonen, 1997; Vesanto et al., 2000) for the entire data set (91 seizures) to inspect for possible clustering. We used the full data set for this inspection, since SOM are known to perform best when large amounts of data are used and the spanning feature space is densely sampled. Based on the result, we returned to step 1 and again varied the feature selection and parameters, followed by a new SOM (step 2). This iterative, heuristic procedure was repeated until we were satisfied with the results of both the steps, quantifying their performance using the k-factor (step 1) and the SOM (step 2).

Classification and Validation

The simplest classification algorithm is thresholding of some relevant feature value—the crossing of such threshold is then defined as "detection." The major drawback of such algorithm is the proper definition of the threshold. This becomes even more complicated when several signals and/or features have to be integrated, each with its own weighting function according to the individual information contribution. Therefore, in this study, we applied a more advanced classifier, SVM (e.g., Cristianini and Shawe-Taylor, 2000; Mueller et al., 2001; Schölkopf, 1998).

The power of the SVM-based classification system (see schematic overview in Fig. 1) was assessed by cross-validation, adopting a seizure-based leave-one-out training and testing procedure. Here, one of the seizures was used as a test set, whereas all other seizures were used for training. This procedure was repeated using each seizure as test set exactly once. By such a design, all data can be used for training and testing, without overlap between training and test sets that could lead to overfitting (Bishop, 1995). The detection power was then computed as the number of correct classifications divided by the total number of test trials (Mehring et al., 2003).

For classification, the normalized feature data were exported to the LIBSVM data format and processed using the software package LIBSVM 2.4 (Chang and Lin, 2001). In this seven class SVM, the radial basis function kernel was applied. The seven classes consisted of the six seizure morphologies (ictal data, cf. Table 1) and one nonictal class. The SVM parameters were estimated once, on the first training set in the leave-one-out procedure, using threefold cross-validation by splitting the training set into three subsets, and using two of them for SVM-training and one for testing—i.e., iteratively as in the leave-one-out procedure. The appropriate weighing of seizure to no-seizure examples in the data was obtained using heuristics, starting from equal weighing between the two classes and changing weight emphasis iteratively to optimize classification performance. We found that favoring nonictal to ictal data in the training of the SVM while determining the support vectors by a ratio 8:1 gave optimal results. This weighing influences the cost-evaluation of the quality during calculation of the optimal margin and determination of the respective support vectors.

A "detection" was assigned when at least three samples of feature data in a 5 seconds sliding window rated as "ictal" by the SVM. A seizure was rated as correctly detected if at least one detection was made in the expert-defined seizure duration, i.e., the time during which the initial seizure morphology was judged prominent in the EEG by the expert. Any change in the ictal pattern was defined as an end of the seizure-period that should be detected. Detections elsewhere, but also excluding the seizure duration following the initial EEG patterns, in the EEG data analyzed were counted as false positives. This procedure tends to underestimate the detection power and overestimate the false-positive rate, since seizures overlooked by the expert and seizures detected by the algorithm earlier than by the expert (or even predicted) are counted as false positives. Yet, we found such strict quality criterion justified for an unambiguous validation of the algorithm and necessary to analyze ictal-morphology dependent performance (cf. Fig. 5). Only in a second stage did we relax the temporal criterion to estimate the possible bias introduced by rejecting early detections (i.e., detections preceding the initial onset of the ictal pattern in the EEG by less than 2.8 seconds) by the algorithm (cf. Fig. 6).

RESULTS

Seizure Morphologies and Features: High Variability

In a first step, we analyzed the variability of the different seizure morphologies (cf. Table 1) and the degree to which it was reflected in the extracted features (cf. Table 2). Figure 2 shows two representative examples of seizure morphologies (Fig. 2A: rhythmic beta activity, Fig. 2C: runs of polyspikes) and the corresponding feature patterns (Figs. 2B and 2D). Observe that distinct patterns of clearly changing feature value distributions are visible for each seizure type, with the probability of finding such distributions by chance showing a clear drop to P-values $<10^{-4}$ near the EEG-expert defined seizure onset for most of the investigated features (cf. Figs. 2B and 2D). Yet, the considerable differences in the time courses of the individual feature value profiles suggest to use more than one feature simultaneously to reliably identify ictal activity.

Morphology-Based Clustering

An automatic morphology class assignment is possible using the information provided by the extracted feature value distributions and the result of the clustering analysis (cf. Feature Value Distributions and Optimizations section). To quantify the possible separability of the data, we computed the k-factors for all seizure morphologies (cf. Table 1) and all features (cf. Table 2). This provides a measure of the distance between the means of the two populations (i.e., ictal vs. nonictal) in relation to the respective variances. The mean k-factors for all features and all morphologies are shown in Fig. 3. Observe that different features have a quite diverse

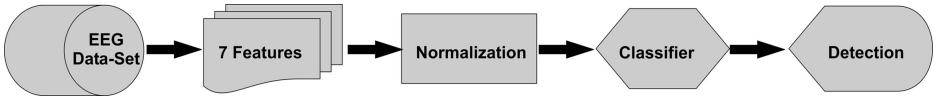

FIGURE 1. Overview of the proposed automatic seizure detection system. The EEG data (cf. Table 1) were first analyzed by extracting seven different features (cf. Table 2), which were normalized using a rank order based sliding normalization. These data were then classified in a leave-one-out cross-validation approach, using a seven class SVM with a radial basis kernel. The output of the SVM was integrated over a sliding window, and the detection of seizure events was returned to the user. For details see Methods sections.

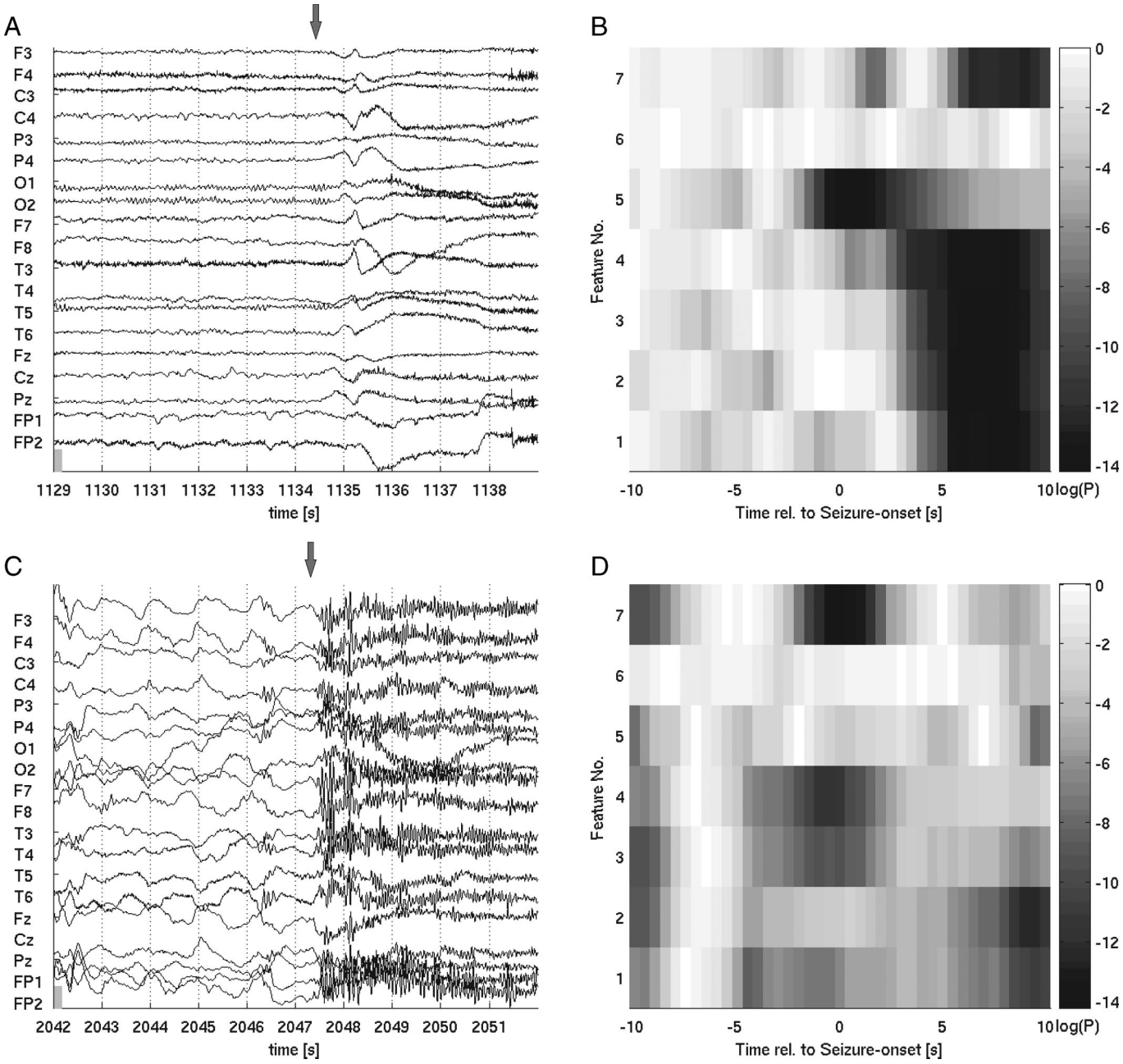

FIGURE 2. Two example seizure morphologies (**A**: Beta, **C**: Polyspikes) and the associated patterns of rank sum normalized feature data (**B**, **D**). The **left** column (**A**, **C**) shows the EEG in a common average reference montage from 5 seconds before until 5 seconds after seizure onset as defined by the EEG expert. The height of the scale bar (**bottom**, **left**) is 10 μV. Onset of ictal patterns are marked with gray arrows. The **right** column (**B**, **D**) shows the temporal evolution of the rank sum probabilities (*P*-values, shown in a logarithmic scale) for each feature (cf. Table 2) for the EEG examples over the time span shown (**A**, **C**). Darker regions indicate a higher probability for the respective feature reflecting a change in signal composition. This change is exploited here for seizure detection, since an emerging seizure will be reflected by changes in the respective feature values. These examples illustrate the usefulness of different features for detecting different seizure morphologies. Moreover, they provide a first indication of the expected latency of possible seizure detection.

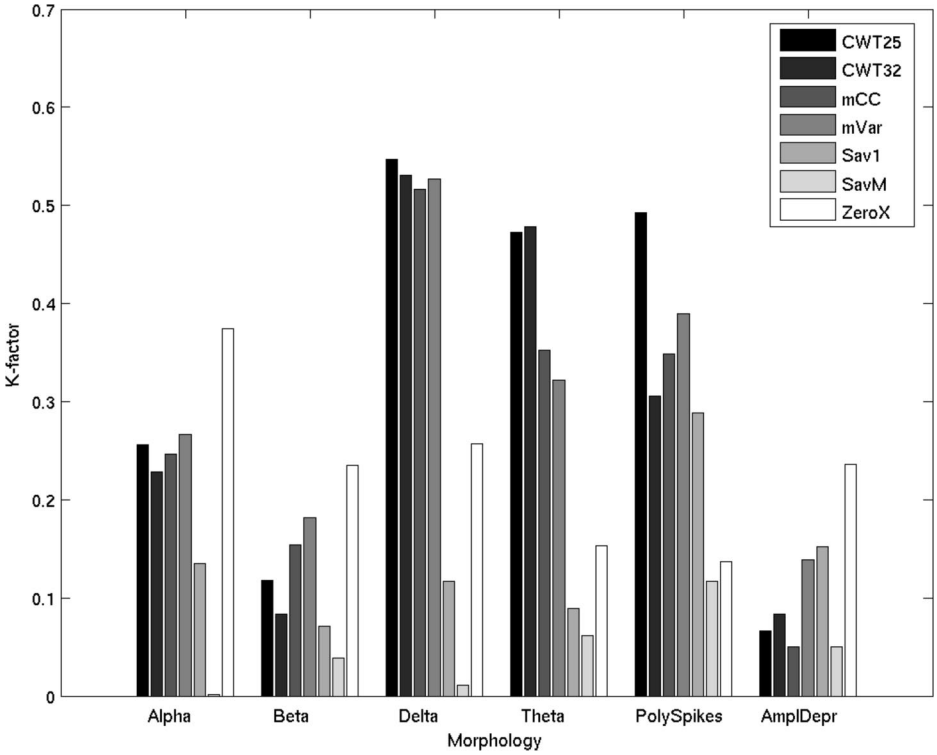

FIGURE 3. *K*-factors for all seizure morphologies (cf. Table 1) and features (cf. Table 2). Gray values represent features (inset, abbreviated as in Table 2). Groups of seven bars represent the *k*-factor distribution, measuring the separability between ictal and nonictal EEG epochs, for different seizure morphologies. The higher the *k*-factor, the better the expected separability. Observe that different features have quite different separation efficacy for different seizure morphologies. This high variability of *k*-factors, depending on seizure pattern, suggests to use multiple features simultaneously to identify ictal activity.

efficacy for separating seizures from nonseizure data, depending on seizure morphology. For example, the CWT25 feature offers most information for separating seizures form normal EEG activity for delta, theta and polyspikes seizures, but is not very useful for identifying seizures characterized by amplitude depression. Conversely, the ZeroX feature provides good separation for seizures with a rhythmic alpha pattern, but much less so for rhythmic theta patterns. This high variability of the *k*-factors depending on seizure pattern once more suggests to use different features for different seizure morphologies, or to use multiple features simultaneously, to become independent of seizure type.

Self-organizing maps are a powerful tool for visualizing high-dimensional data. They were used here to detect a possible clustering of seizure data that cannot be detected using variance explanation maximizing methods like principal component projection (Kaski, 1997). Such clustering may yield an estimate of the number of classes necessary when using a multiclass detection approach. Figure 4 shows a unified distance matrix projection of ictal and nonictal feature values, with labels indicating the voting behavior of the SOM-nodes ("neurons"). The clustered distribution of morphology labels over the map suggests to differentiate between at least two different classes of seizures. The relative frequencies of seizure morphologies in the clusters suggests that these clusters mainly separate rhythmic alpha, delta, and beta patterns (left: A, D, B) from polyspikes (right: P). Moreover, the shape of the large cluster on the left is suggestive of two subclusters, one with alpha and delta (top left), the other with beta (and some alpha) near the center of the map. Theta and amplitude-depression (*T*, *R*) take intermediate positions, with their nodes appearing next to (or even within) both main clusters. Most nodes in between the clusters and in the lower half of the map represent nonictal activities. The positions of the various seizure morphologies in the map suggest that rhythmic alpha and beta patterns and, especially, amplitude-depression should be more difficult to reliably detect and classify, as their nodes are mainly surrounded by nonictal nodes and are situated in regions with low internode distances. By contrast, the other morphologies (rhythmic delta, theta, and polyspikes) should be easier to detect, because their nodes tend to cluster at the top of the map, the furthest away from the nonictal nodes.

Not only the expected difficulty of detection and separation of the different ictal morphologies can be estimated from the SOM-map, but also common properties of the various classes are reflected by the observable neighborhoods. For instance, ictal rhythmic alpha and delta patterns are observed near each other within a subcluster, reflecting their common origin as cortically generated rhythms. Generally, the transition between the ictal frequency bands is a reason for the observed clustering. Thus, the clustering of ictal patterns as suggested by Fig. 4 typically concerns seizure morphologies that are closely related from a neurophysiological point of view.

Seizure Detection Performance Using SVM Classifier

We analyzed the performance of the proposed seizure detection system (cf. Fig. 1) with regard to (a) detection of a given pattern as an ictal event, and (b) classification of a pattern with regard to the different morphologies listed in

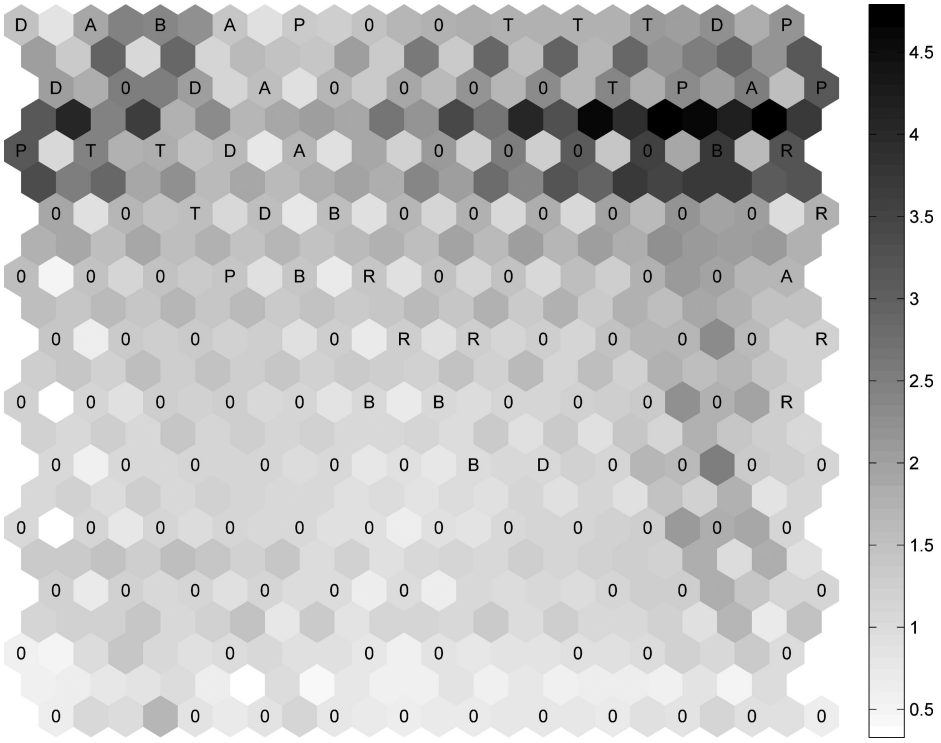

FIGURE 4. Clustering of seizures according to their similarity in feature space, shown in the unified distance matrix of an SOM projection with a sheet topology. Labels in the nodes represent the voting behavior of the SOM-"neurons" for the different seizure morphologies, where "0" indicates a vote for the no-seizure class and "A, B, D, T, P, R" refer to alpha, beta, delta, theta, polyspikes and amplitude-depression, respectively. The voting of the nodes was weighted with the relative abundance of class instances. The distance between SOM-nodes (dissimilarity between the "voting neurons") is gray coded as indicated; the gray value of a node itself corresponds to the average distance to the surrounding nodes. Several clusters and subclusters can be discerned; for a more-detailed description we refer to the main text.

Table 1. Results show that both detection and classification can be achieved at high performance, despite a considerable interpatient and intramorphology variability. Thus, the features extracted from the EEG data are able to capture the wide spectrum of epileptic seizure patterns.

To integrate the information obtained by using a seven-dimensional description (cf. features in Table 2) of the data while using six classes to represent the different seizure morphologies (cf. Table 1), we used a multiclass nonlinear SVM with a radial basis function kernel to classify the data. As shown in Fig. 5, the system reaches a very high correct detection rate (Fig. 5A, 85%–100%), together with low false alarm rates (Fig. 5B, 0.2–0.4 false alarms per hour for rhythmic alpha, beta, delta, theta and polyspike classes, and approximately 1.6 for amplitude-depression). The distinctly higher amount of false positives in the latter case, which confirms the prediction from the SOM-map (cf. Fig. 4 and Morphology-Based Clustering section), is most likely due to the inherently relative nature of the definition of amplitude-depressions in the EEG, combined with the high variability in underlying EEG frequencies, and with the lower specificity of this pattern for ictal activity related to physiologically occurring periods with amplitude depression of EEG background activity, e.g., related to changes in vigilance and eye openings. Figure 5A does not provide any evidence for a differential detection performance depending on the duration of the ictal events (cf. Table 1), thereby arguing against a possible bias against short seizures that might have been introduced by excluding subclinical seizures from the database.

Also the distribution of false alarm rates over EEG data sets (Fig. 5C) is encouraging, with a median better than 0.3 false alarms per hour and only few outliers at higher values. To confirm the false alarm rate obtained here using the data presented in Table 1, we additionally evaluated the detection system on approximately 24 hours of seizure free data for each of the 57 patients (in total roughly 1,360 hours). The resulting false alarm rate distribution (not shown here) was highly similar to the one obtained on the dataset described in Table 1. Therefore, we restrict ourselves to a detailed report of the findings from the 43 hours data set.

The detection latency is of high interest for an automatic online seizure detection system: clearly, a small latency window would offer time for therapeutic intervention while the seizure is evolving, and allow to perform tests while the seizure is still ongoing. Even a short warning period before the onset of behavioral changes of the patient might be possible for a detection system with a low enough latency. The distribution of latencies of the automatic detection system is shown in Fig. 5D. Positive latencies in the graph signify a delayed detection by our algorithm when compared with the seizure onset defined by the EEG-experts, negative latencies signify an earlier detection by our detection system. Interestingly, the latency distribution is close to Gaussian, with a mean delay of +1.6 seconds (median, +2.0 seconds) and a standard deviation of 2.8 seconds. That is, detection is achieved almost instantly (for most of the seizures within 2 seconds) after the expert-defined seizure onset, although only EEG information up to this time point was used for detection. If we assume that (1) the EEG-expert and the automatic system operate in a statistically independent manner (which seems reasonable) and (2) the EEG-experts exhibit a temporal jitter in the range of 1 to 2 seconds in their seizure onset definition (which also seems reasonable), this would suggest that the temporal jitter of the automatic seizure detection

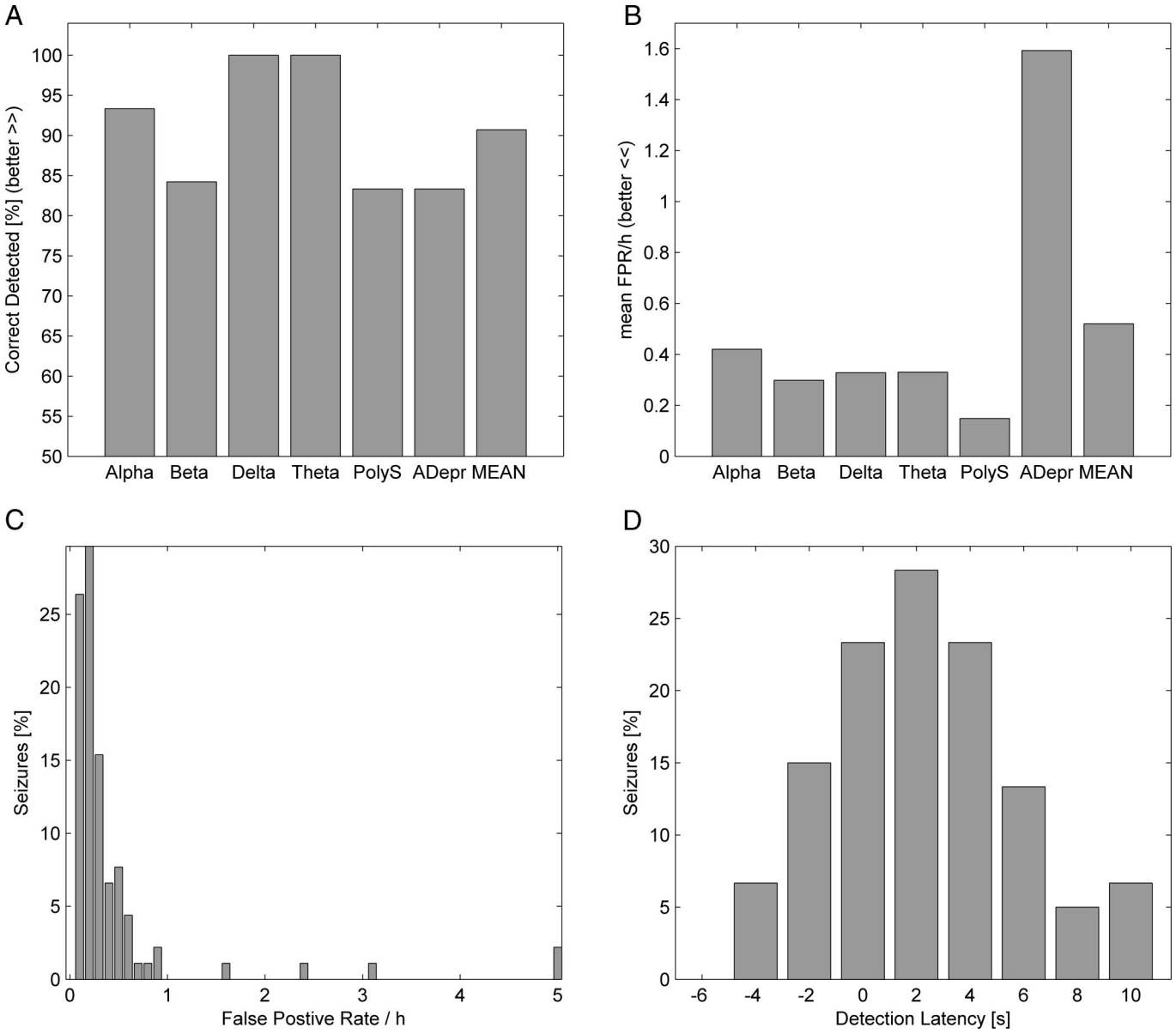

FIGURE 5. Performance of the proposed seizure detection system (cf. Fig. 1). **A**, Percentage of correctly detected seizures per morphology. **B**, False alarm rates per hour as a function of seizure morphology (median: 0.21 FP/h, mean: 0.45 FP/h). **C**, Distribution of false alarm rates per EEG data block. Observe the high correct detection rate, together with low false alarm rates, both per seizure morphology and per EEG data block. **D**, Distribution of latencies with respect to seizure onset defined by EEG-expert (mean, +1.6 seconds; SD, 2.8 seconds). Positive latencies signify a delayed detection by the automatic system, negative latencies signify an earlier detection.

system is comparable with that of its human counterpart. Usually, human experts also take subsequent EEG-segments (especially for rather "unspecific" seizure patterns like amplitude depression) into account in visual EEG review. Unfortunately such a procedure is unfeasible with a moving-window-based automatic seizure detection system, since it would require a kind of bootstrapping procedure over time.

In our performance analysis (cf. Fig. 5), we have thus far adopted the rule that only automatic detections with zero or positive (less than the duration of the initial ictal pattern, c.f. EEG Data section) delay were counted as "correct" detections. In particular, automatic detections with negative delay (i.e., too early) were counted as "false." As Fig. 5D clearly shows, there is indeed a considerable fraction (~21%) of such early, hence as false rejected, automatic seizure detections. Accepting the above-described reasoning concerning the possible temporal jitter of detection, adopting such strict rule of discarding early automatic detections by definition as false would, in fact, be unreasonable. In particular, it would by definition rule out the possibility that the

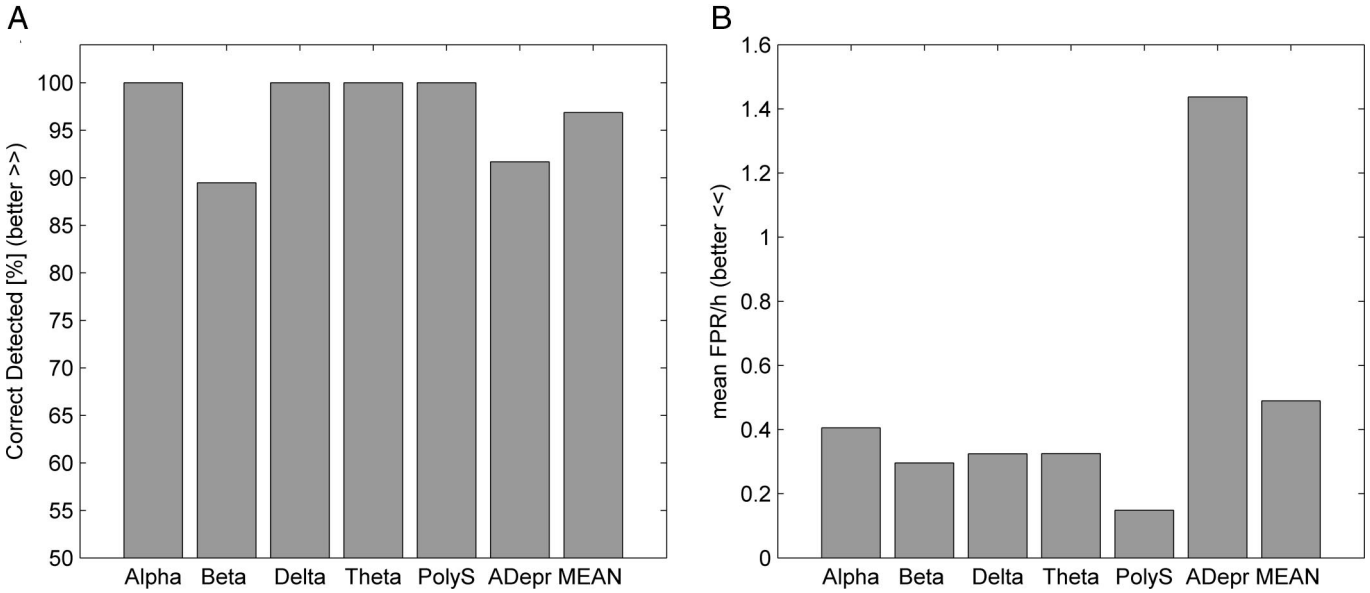

FIGURE 6. Performance of the proposed seizure detection system, with relaxed conditions on detection latency: In addition to the criteria used in the performance analysis in Fig. 5, now also early automatic detections were accepted as "correct" if they preceded EEG-expert detection by less than 2.8 seconds (cf. Fig. 5D). Further explanation in text. **A**, Percentage of correctly detected seizures per morphology. **B**, False alarm rates per hour as a function of seizure morphology. These results should be compared with those of the "stricter" analysis in Fig. 5.

automatic detection system might occasionally reach a judgment earlier than the EEG-expert, within the bounds imposed by the temporal jitter of the expert and the automatic detection system. To investigate the possible consequences of alleviating this strict rule, we recomputed the performance analysis of Figs. 5A and 5B, but now in addition accepted early automatic detections as "correct," provided they preceded the EEG-expert detection by less than 2.8 seconds, as suggested by the temporal bounds of the latency distribution in Fig. 5D. The results of this "time-relaxed" performance analysis are shown in Fig. 6, with each of the panels (Figs. 6A and 6B) representing the "relaxed" version of its "stricter" counterpart (Figs. 5A and 5B). As expected, the correct detection rate even further increased (Fig. 6A, 90%–100%), whereas the false alarm rates remained the same or only slightly decreased (Fig. 6B, down to 1.4 for amplitude-depression).

Feature Ranking Using Linear Classifiers

Finally, we compared the performance of our SVM-based detection system (Fig. 1) with that of a simple feature thresholding algorithm. By this procedure, we wanted to obtain deeper insight into the contribution of each individual feature in seizure detection. Thus, we ranked the features according to their performance using a simple linear classifier (c.f. Table 2, "Feature Rank"). To obtain the feature rank we used the false alarm rate per hour with a fixed amount of true positives (TP). We found that for reasonable high TP values (95%–70%) the rank order of the features were robust; therefore, the exact chosen TP rate within these limits was not crucial for feature ranking and we set the demanded TP rate to 90%. This seems reasonable, since optimal detection performance might be a very ambitious aim for such a difficult task and very low values (i.e., below 70%) would only represent the performance of an oversimplified task.

The ranking we obtained is shown in Table 2. The features described elsewhere (No. 1–3) performed quite good, however, the newly introduced feature No. 4 (mean CC) performed best. The mean CC feature estimates the cross-correlation between electrode pairs and, thus, can quantify spread of synchronized activity between electrodes. It is the only feature in our feature set that directly addresses the spatial spread of seizure activity in the EEG. It has been suggested by Gotman et al. in 1999 that integration of spatial information may reduce false alarm rates significantly. This is confirmed by the rank ordering of the features we used here. Our ranking with respect to performance may thus provide valuable information regarding characteristic properties of features and offer a starting point for further improvement in future seizure detection algorithms.

DISCUSSION

We described a novel procedure for online, real-time automatic seizure detection in human long-term EEG, together with its validation in routine clinical EEG recordings. We found that taking the diversity of seizure morphologies into account drastically improves the seizure-detection performance of the system and is crucial for valid assessment of performance regarding ictal-patterns. Moreover, besides enabling a reliable and early detection, the method facilitates automatic categorization of the prevalent seizure morphologies. We are aware of the inevitable fact that for addition to the dataset used here (cf. Methods, EEG Data section) the

initial ictal pattern had to be identified by the clinical personnel, which could lead to a possible bias against patterns that are difficult to assign to a specific class. While collecting the data, we did not apply any preselect based on the quality of the EEG recording. Only a very small percentage of patterns reviewed for this study were termed "unclear." Thus, we conclude that this potential bias is unlikely to have influenced the performance of the detection system proposed here. In the validation, the method exhibited a high detection power (Fig. 5A) and low false positive rates (Fig. 5B), while operating at relatively low computational costs (for a 10–20 electrode setup, the system operates in approximately 1/7 real time on a standard desktop computer). Moreover, we could confirm the stability of the false alarm rates estimated on the 43 hours data set (cf. Table 1) by additionally evaluating 24 hours long seizure free data for each of the 57 patients used in this study.

In the design of this study, there was a partial overlap between the data set used for the evaluation of the seizure detection performance and the data set used to initially calibrate and implement the features used. Although the validation of the proposed system was performed using independent and overlap-free cross-validation, there might still be a small risk for a bias introduced while developing the feature set used. A complete separation of these data sets, each of them large enough to represent the full variability of initial ictal patterns and patients would have required an independent duplication of the full data set used here. This would have been a tremendous effort compared with the minor potential bias possibly introduced by a partial overlapping between the datasets used for feature development and for performance testing. The danger of such bias was further minimized by using completely different methods for evaluation in the two processes: *k*-factor and SOM for feature set development versus nonlinear SVM for classification. Thus, the proposed seizure detection system seems promising for generalization and application in clinical routine and utilization as an additional tool to alleviate work of electroencephalographers during EEG recordings.

Comparison With Other Automated Seizure Detection Systems

The excellent review of Gotman (1999) offers a good starting point for comparison of the proposed system with established methods for automatic seizure detection. Most systems proposed in the literature have revealed interesting aspects of seizures. Matching the published detection rates, however, was no easy task. Some of the known algorithms have a limitation in that they require adaptation of the algorithm to a specific patient and/or seizure morphology. Such limitations are avoided in the proposed method, which captures different seizure morphologies at once and is not tuned to a specific patient or seizure localization in any way. Also, it does not require a matching template to search for already known seizure signatures, such as mentioned in the approach by Qu and Gotman (1995, 1997). Osorio et al. (1998) reported almost perfect performance of a seizure warning method based on depth electrodes and EcoG. Unfortunately, however, they did not specify the detection delay after seizure onset in the scalp EEG. The delay of our algorithm is very short (Fig. 5D), which in most cases would allow a direct seizure-related alert and possibly in some cases in which semiological seizure onset has an appropriate latency also allow for intervention. Moreover, the present system is based on surface EEG recordings that, besides being noninvasive, are very easy and cheap to obtain, and applicable to a wide range of patients. A comparison with the probably best known, by now fairly old, detection system proposed by Gotman—first published in 1982 and updated several times meanwhile—shows clear advances in a strong increase in the percentage of correctly detected seizures (from 76% to 90%–100%, depending on seizure type; Fig. 5A) and a reduction of false positive rates (from about 1/h to 0.2–0.5/h, depending on seizure type, with the exception of amplitude depression that remains at 1.6/h; Fig. 5B). When taking potential jitter in the visual, expert-based marking of the onset of the ictal pattern into account and, therefore, relaxing the boundaries for the evaluation (i.e., by allowing correct detections also a few second before the marked onset of the initial ictal pattern) of correct detections we can reach very high correct detection rates (Fig. 6A). As expected the false alarm rates are only influenced negligibly by this (Fig. 6B). Although promising, an independent validation of these findings seems to be difficult, since a bootstrapping procedure or a validation on an independently created, different data set of more or less the same size might be needed.

A further increase in detection performance could be achieved by another, additional procedure. Since some ictal patterns (especially amplitude depression, where the detection performance of our system would profit most) are generally followed by other ictal patterns, a detection system based on detected ictal sequences could reach higher correct detection performance. Such an "ictal grammar" based system would of course increase the detection latency. When taking the average duration of an initial ictal pattern used here into account, the detection latency would increase by about 8 to 10 seconds. This might be good enough for an offline evaluation of the data, but seems unacceptable for intervention purposes.

However, even for the direct approach, which is not taking sequences of ictal patterns into account, a direct comparison of the numerical values for the detection performance is difficult, because of the different data selections in the various studies. In this context, it would be highly desirable to have the possibility to compare the different algorithms on the basis of their performance on a single benchmark data base, such as the one used in the present study (Dittrich et al., 2003). In any case, since our algorithm was trained and validated on long-term EEG recordings obtained during routine clinical application, the improvements achieved by our method would seem to be favorable for its application in similar settings, or when long-term recordings with durations of days to weeks have to be analyzed off-line.

Recent work by Saab et al. (2005) reported good seizure-detection performance comparable with ours in a huge EEG data-set. In comparison with our approach, their system additionally exploited a user-tuneable detection thresh-

old, and was paired with a higher detection latency. Another, very recent, publication (Hopfengaertner et al., 2007) showed comparable correct detection rates and false alarm rates using a method based on frequency analysis of the EEG. There, however, the good performance came with very high detection delays (10–44 seconds) compared with our method (<5 seconds, Fig. 5D), which therefore seems to be favorable, especially when considered for online detection. Finally, the work of Faul et al. (2005) on data of neonates nicely illustrates the difficulties of generalization of seizure detection approaches from adult to neonate EEG. The seizure-detection problem for neonates still seems to be unresolved.

Classification of Different Seizure Morphologies

The automated identification of ictal EEG patterns into different seizure morphologies may have additional clinical value as EEG patterns of similar topography may allow to infer the seizure generators (Ebersole and Pacia, 1996; O'Brien et al., 1996) and, thereby, contribute to the identification of the epileptogenic zone in patients who are candidates for epilepsy surgery. As using the SOM-based analysis (Fig. 4), pathophysiologically similar patterns appeared clustered for the extracted features. Related pattern pairs like beta and polyspikes, and alpha and delta ictal patterns were found grouped near to each other—providing valuable hints regarding the generation mechanisms involved.

The SOM as a classic pattern recognition tool served as a strong indicator for using multidimensional and multiclass descriptions for seizure detection. Moreover, it showed how the high variability of different seizure morphologies was reflected by the features used in our approach. Also the *k*-factor, a measure for distribution separability, suggested to rely on a multidimensional approach. By using a feature ranking approach based on the performance of a simple linear thresholding algorithm, we quantified the contribution of each feature used in this study to the overall detection performance. We chose such simple comparison, since a full evaluation like the one presented by van Putten et al. (2005) would be beyond the scope of this article. There, features measuring "asymmetry" of EEG activity performed best for seizure detection. The feature that performed best in our study was the mean coefficient of correlation between electrode pairs (mean CC), which essentially captures the spatial spread of seizure activity patterns in the EEG.

SVMs are known to be powerful model building algorithms and their superior integration of more than one dimension was demonstrated again here. Their also well-known susceptibility to different scaling of the data was bypassed by using the sliding rank sum test. This has the advantageous properties of, first, removing any offset in the data and, second, being a robust estimator for changes in a signal, which can be directly converted to a probability. In comparison with the patient-specific detection system proposed by Shoeb et al. (2004), our system reached a better performance, even though it was used in a generic (i.e., not patient-specific) setting—this might be a consequence of the inclusion of multiple features into our system.

The amplitude depression seizure class showed the highest false positive rate (Fig. 5B). This might be taken to indicate that the proposed system is able to detect them only at a costly trade-off. This drop in performance for amplitude depression seizures might be inherent to the unspecific nature of this seizure pattern (which is "relative" by definition) and/or to the associated high variability in underlying EEG frequencies. Moreover, unfortunately, high-quality data for amplitude depression morphologies were not abundant in our data base. In fact, the examples included in the present study contained various disturbing events in the nonictal EEG data, among them even subclinical seizures, electrode and movement artifacts, and problems with the recording system. Thus, we did not select the data in a way to avoid real world problems in clinical EEG recording setups. Thus, the problem of distinguishing a widespread reduction in the amplitude of EEG signals from spontaneous fluctuations, which occur in the interictal record (cf. Alarcon et al., 1994) due to its lack of specificity when compared with other ictal patterns may limit not only visual inspection but also automated analysis systems in their performance to classify these events as ictal or unrelated to epileptic activity.

OUTLOOK

Further improvement of the algorithms presented here may result from the additional integration of spatial relationships between the various EEG channels analyzed in the algorithm. Additionally, the integration of blind source separation techniques as a first stage for filtering the EEG data and removal of artifacts might yield a further increase in performance (Meier et al., 2005).

In view of the high detection performance and the overall very low false positive rates (Fig. 5), together with the relative low computational demands (the system operates in approximately 1/7 real time on a standard desktop computer for a 10–20 electrode system), the proposed automatic seizure detection system seems to be very promising for application in clinical routine. A user friendly standalone evaluation version is straightforward to implement. It might be profitably used as an additional tool to alleviate work of electroencephalographers during the EEG recordings. By use of such system, the data volume that would have to be reviewed can be reduced by a considerable amount. Also a possible application in Tele-EEG, studied by Holder et al. (2003), as a tool for preselection of interesting EEG epochs before transmitting the data over a phone line could be promising. Finally, the low latency of detection (Fig. 5D) after seizure onset in the EEG might allow for an application as a warning tool in patient monitoring and enable to alert medical personal to seizures while they are still ongoing, including cases in which there are no overt changes in the behavior of the patient. This might even open an interesting window for automated diagnostic systems like the early application of tracers for ictal SPECT (Lee et al., 2006) or possibly even yield useful triggers for intervention systems aiming at terminating upcoming or ongoing ictal activity.

ACKNOWLEDGMENT

The authors thank Armin Brandt and Carolin Gierschner for supplying the EEG long-term data from the Freiburg Epilepsy Centre.

REFERENCES

Alarcon G, Binnie C, Elwes R, Polkey C. Power spectrum and intracranial EEG patterns at seizure onset in partial epilepsy. *Electroencephalogr Clin Neurophysiol*, 1994;94:326–337.

Alhoniemi E, Himberg J, Parviainen J, Vesanto J. SOM Toolbox version 2. 0beta. http://www.cis.hut.fi/projects/somtoolbox/. GNU Public Licence; 2001.

Battiston JJ, Darcey TM, Siegel AM, et al. Statistical mapping of scalp-recorded ictal EEG records using wavelet analysis. *Epilepsia* 2003;44: 664–672.

Bishop CM. Neural Networks for Pattern Recognition. Oxford: Clarendon Press; 1995.

Bikson M, Hahn PJ, Fox JE, Jefferys JGR. Depolarization block of neurons during maintenance of electrographic seizures. *J Neurophysiol* 2003; 90:2402–2408.

Chang CC, Lin CJ. LIBSVM: a library for support vector machines. Software available at http://www.csie.ntu.edu.tw/~cjlin/libsvm.

Cristianini N, Shawe-Taylor J. An Introduction to Support Vector Machines and other kernel-based learning methods. UK:The Press Syndicate of the University of Cambridge; 2000.

D'Arcangelo G, D'Antuono M, Biagini G, et al. Thalamocortical oscillations in a genetic model of absence Seizures. *Eur J Neurosci* 2002;16:2383–2393.

Daubechies I. Ten lectures on wavelets, CBMS, *SIAM* 1994;61:198–202, 254–256.

Dittrich H, Brandt A, Meier R, et al. Relevanz der klassifikation iktualer muster in einer EEG-datenbank für die entwicklung und evaluation von algorithmen zur automatisierten detektion von anfallsmustern. *Klin Neurophysiol* 2003;34. DOI: 10.1055/s-2003–816428.

Dzhala VI, Staley KJ. Transition from interictal to ictal activity in limbic networks in vitro. *J Neurosci* 2003;23:7873–7880.

Ebersole JS, Pacia SV. Localization of temporal lobe foci by ictal EEG patterns. *Epilepsia* 1996;37:386–399.

Echauz J, Padovani D, Esteller R, et al. *Median-based Filtering Methods for EEG Seizure Detection*. Atlanta, GA, USA. First Joint BMES/EMBS Conference: Serving Humanity, Advancing Technology; 1999.

Esteller R, Vachtsevanos G, Echauz J, et al. Accumulated energy is a state-dependent predictor of seizures in mesial temporal lobe epilepsy. *Epilepsia* 1999;40:173–173.

Esteller, R. *Detection of Seizure onset in Epileptic Patients from Intracranial EEG Signals*. PhD thesis, School of Electrical and Computer Engineering; 1999.

Faul S, Boylan G, Connolly S, et al. An evaluation of automated neonatal seizure detection methods. *Clin Neurophysiol* 2005;116:1533–1541.

Gotman J. Automatic Recognition of Epileptic Seizures in the EEG. *Electroencephalogr Clin Neurophysiol* 1982;54:530–540.

Gotman J. Automatic detection of seizure and spikes. *Clin Neurophysiol* 1999;16:130–140.

Holder D, Cameron J, Binnie C. Tele-EEG in epilepsy: review and initial experience with software to enable EEG review over a telephone link. *Seizure* 2003;12:85–91.

Hopfengärtner R, Kerling F, Bauer V, Stefan H. An efficient, robust and fast method for the offline detection of epileptic seizures in long-term scalp EEG recordings. *Clin Neurophysiol* 2007;118:2332–2343.

Ishikawa Y, Mochimaru F. 2002 Wavelet theory-based analysis of high-frequency, high-resolution electrocardiograms: a new concept for clinical uses. *Progress in Biomedical Research* 2002;7:179–184.

Kahn Y, Gotman J. Wavelet based automatic seizure detection in intracerebral electroencephalogram. *Clin Neurophysiol* 2003;114:898–908.

Kaski S. *Data Exploration Using Self-Organizing Maps*. PhD-Thesis, Helsinki University of Technology, Neural Network Research Centre; 1997.

Kohonen T. *Self-Organizing Maps*. Springer Series in Information Sciences; 1997.

Lee SK, Lee SY, Yun CH, et al. Ictal SPECT in neocortical epilepsies: clinical usefulness and factors affecting the pattern of hyperperfusion. *Neuroradiology* 2006;48:678–684.

Le Van Quyen M, Martinerie J, Baulac M, et al. Anticipating epileptic seizures in real time by a non-linear analysis of similarity between EEG recordings. *Neuroreport* 1999;10:2149–2155.

Le Van Quyen M, Martinerie J, Baulac M, et al. Spatio-temporal characterizations of non-linear changes in intracranial activities prior to human temporal lobe seizures. *Eur J Neurosci* 2000;12:2124–2134.

Le Van Quyen M, Martinerie J, Navarro V, et al. Anticipation of epileptic seizures from standard EEG recordings. *Lancet* 2001;357:183–188.

McSharry P, He T, Smith L, et al. Linear and non-linear methods for automatic seizure detection in scalp electro-encephalogram recordings. *Med Biol Eng Comput* 2002;40:447–461.

Mehring C, Rickert J, Vaadia E, et al. Inference of hand movements from local field potentials in monkey motor cortex. *Nature Neurosci* 2003; 6:1253–1254.

Meier R, Schulze-Bonhage A, Cichocki A, Aertsen A. *Artifact removal from the EEG—Blind source separation and complex artifacts*. In: Zimmermann H, Krieglstein K, eds. Proceedings of the Sixth Meeting German Neuroscience Society, 30th Göttingen Neurobiology Conference Neuroforum 1/2005, Suppl: 466A.

Mueller K-R, Mika S, Raetsch G, et al. An introduction to kernel-based learning algorithms. *IEEE Trans Neuronal Networks* 2001;12:181–201.

Murro AM. Computerized seizure detection of complex partial seizures. *Electroenceph Clin Neurophysiol* 1991;79:330–333.

Netoff T, Schiff S. Decreased neuronal synchronisation during experimental seizures. *J Neurosci* 2002;22:7297–7307.

O'Brien TJ, Kilpatrick C, Murrie V, et al. Temporal lobe epilepsy caused by mesial temporal sclerosis and temporal neocortical lesions. A clinical and electroencephalographic study of 46 pathologically proven cases. *Brain* 1996;119:2133–2141.

Osorio I, Frei M, Wilkinson S. Real-time automated detection and quantitative analysis of seizures and short-term prediction of clinical onset. *Epilepsia* 1998;39:615–627.

Osorio I, Frei M, Giftakis J, et al. Performance reassessment of a real-time seizure-detection algorithm on long ECoG series. *Epilepsia* 2002;43: 1522–1535.

Press WH, Teukolsky SA, Vetterling WT, et al. *Numerical Recipes in C—The Art of Scientific Programming*. 2nd edn. Cambridge, MA: Cambridge University Press, 1992.

Qu H, Gotman J. A seizure warning system for long-term epilepsy monitoring. *Neurology* 1995;45:2250–2254.

Qu H, Gotman J. A patient-specific algorithm for the detection of seizure onset in long-term EEG monitoring: possible use as a warning device. *IEEE Trans Biomed Eng* 1997;44:115–122.

Schiff SJ, Aldroubi A, Unser M, et al. Fast wavelet transformation of EEG. *Electroencephalogr Clin Neurophysiol* 1994;91:442–455.

Schölkopf B. Support-vektor-lernen. In Hotz G, et al. eds., *Ausgezeichnete Informatikdissertationen.* Stuttgart: Teubner, 1998;135–150.

Sharbrough FW. Scalp-recorded ictal patterns in focal epilepsy. *J Clin Neurophysiol* 1993;10:262–267.

Shoeb A, Edwards H, Connolly J, et al. Patient-specific seizure onset detection. *Epilepsy Behav* 2004;5:483–498.

Saab ME, Gotman J. A system to detect the onset of epileptic seizures in scalp EEG. *Clin Neurophysiol* 2005;116:427–442.

Vesanto J, Himberg EA, Parhankangas J. SOM Toolbox for matlab 5. Report A57. Espoo, Finland: Helsinki University of Technology, Neural Networks Research Centre, 2000.

Van Putten MJ, Kind T, Visser F, et al. Detecting temporal lobe seizures from scalp EEG recordings: a comparison of various features. *Clin Neurophysiol* 2005;116:2480–2489.

